Heat Mass Transfer (2016) 52:1037–1049
DOI 10.1007/s00231-015-1619-y

ORIGINAL

Simulation and optimization of Al–Fe aerospace alloy processed by laser surface remelting using geometric Multigrid solver and experimental validation

Moisés Meza Pariona[1,2] · Fabiane de Oliveira[1] · Viviane Teleginski[2] · Siliane Machado[2] · Marcio Augusto Villela Pinto[3]

Received: 14 August 2014 / Accepted: 25 June 2015 / Published online: 10 July 2015

Abstract Al–1.5 wt% Fe alloy was irradiate by Yb-fiber laser beam using the laser surface remelting (LSR) technique, generating weld fillets that covered the whole surface of the sample. The laser-treatment showed to be an efficient technology for corrosion resistance improvements. In this study, the finite element method was used to simulate the solidification processes by LSR technique. The method Multigrid was employed in order to reduce the CPU time, which is important to the viability for industrial applications. Multigrid method is a technique very promising of optimization that reduced drastically the CPU time. The result was highly satisfactory, because the CPU time has fallen dramatically in comparison when it was not used Multigrid method. To validate the result of numerical simulation with the experimental result was done the microstructural characterization of laser-treated layer by the optical microscopy and SEM techniques and however, that both results showing be consistent.

✉ Moisés Meza Pariona
mmpariona@uepg.br

Fabiane de Oliveira
faboliveira@uepg.br

Marcio Augusto Villela Pinto
marcio_villela@ufpr.com.br

[1] Department of Mathematic and Statistic, State University of Ponta Grossa (UEPG), Ponta Grossa, PR, Brazil

[2] Graduate Program in Engineering and Materials Science, State University of Ponta Grossa (UEPG), Ponta Grossa, PR, Brazil

[3] Department of Mechanical Engineering, Federal University of Paraná (UFPR), Curitiba, PR, Brazil

1 Introduction

1.1 Laser-treated surface

The laser surface remelting (LSR) technique has been extensively studied over the last few years, especially aiming to enhance surface microhardness and corrosion resistance, since LSR produces microstructural modifications resulting from localized heating and extremely high cooling rates, this is supported by Pariona et al. [1].

In recent articles published by authors Pariona et al. [1–3], they studied the processes of casting of Al–1.5 wt% Fe alloy and the samples treated by laser surface melting (LSM). As well as, the characterization of laser-treated layer using different techniques was performed, among the techniques that they used were: optical microscopy, SEM, atomic force microscopy, low-angle X-ray diffraction and microhardness. Finally, the characterization of LSM layer and untreated was done by different techniques of corrosion. The following are some of the results are described: An homogenous microstructure was verified as a result of rapid solidification; the LSR technique was successfully established to improve the surface properties of Al–1.5 wt% Fe alloys in relation to the substrate alloy; metastable phases in the samples treated by LSM were identified; LSM surface behaved more chemically stable phase in relation to the untreated sample, i.e. improved passive/oxide film after LSR treatment, which could serve as an effective barrier against corrosion attack in aggressive sulfuric acidic environments; in the cyclic polarization curves of the untreated sample it was observed greater area of hysteresis loop i.e. higher susceptibility to corrosion than for the laser-treated sample; and LSR process indeed has an influence on surface film modification, which results in higher corrosion resistance.

1.2 Mathematical model at laser-treated

The authors Mikazaki and Giedt [4] studied the temperature distribution around and the heat flow from a cylinder moving through an infinite plate, according to the analytical treatment of partial differential equation. These authors were pioneers, thus, by first time this study was applied to electron beam welding, to study heat flux distributions around an elliptical cylinder moving through an infinite plate, also proposed these authors electron beam welding full penetration model and their studies were compared with experimental results, being the comparison was satisfactory.

According to Liu et al. [5], the shaped high power laser beam was employed to simulate the thermal loading on large engine parts like pistons and cylinder heads. Experimental and numerical simulation methods were used to study the transient temperature field and helped to the analysis of the thermal fatigue on pistons further, which showed to be competent in the thermal fatigue tests of workpieces with complex configuration.

Other authors like Cho et al. [6] have contributed recently on this subject. They affirmed that one of the goals of laser welding research is to determine optimal conditions by analyzing the effects of the welding conditions from the perspective of the process, metallurgy and mechanics. In welding simulations, it is important to formulate reliable models based on actual welding phenomena. However, practical welding involves complex multiple simultaneous physical phenomena, such as heat transfer, diffusion and electromagnetism, as well as solid, liquid, gas and plasma phases. Thus, many simplifying assumptions are adopted to study physical phenomena separately (Bessroura et al. [7]; Bertelli et al. [8]; Abderrazak et al. [9]). The mathematical models that appear in these problems, in general, do not present analytical solutions. The numerical method was used to turn the continuous model into a discrete model.

A 3D Cartesian coordinate system was set on the workpiece, being the x-axis along the moving welding direction with v speed, y-axis along the width, z-axis along the thickness direction, and the origin located on the workpiece surface. The transient heat conduction equation, which it was proposed by Yilbas et al. [10] and it is written as

$$\rho\frac{\partial(CpT)}{\partial t} = \frac{\partial}{\partial x}\left(k\frac{\partial T}{\partial x}\right) + \frac{\partial}{\partial y}\left(k\frac{\partial T}{\partial y}\right) + \frac{\partial}{\partial z}\left(k\frac{\partial T}{\partial z}\right) + (1-rf)I_0\exp\left(-\frac{x^2+y^2}{a^2}\right)\exp\left(-\delta z\right) \quad (1)$$

where x, y and z are the vertical, depth and horizontal coordinates, respectively, ρ is the density, c_p is the specific heat, k the thermal conductivity, r_f the surface reflectivity, I_o is the laser peak intensity, δ is the absorption depth, t is time, and a is a parameter that determines the laser application form assumed as Gaussian (Gaussian parameter).

1.3 Multigrid methods

To reduce the discretization error in these problems very refined meshes are necessary, which generates large systems of equations. The resolution of these systems through direct or iterative methods requests a large amount of processing time by the Central Processing Unit (CPU). The convergence rate, which is high at the beginning of the iterative process, decreases slightly by increasing the number of iterations, study conducted according to various authors, Briggs et al. [11] and Wesseling [12].

Nowadays, Multigrid method (MG), proposed originally by Fedorenko [13], is one of the most used numerical methods in the solution of systems of equations. According to Briggs et al. [11] this method consists on the transference of information among a refined grid, in which the numerical solution is desired, and coarse auxiliary grids, where numerical smoothers (numerical iterative methods to solve systems of equations, called here as solvers) are more efficient. The transference of information between two meshes is done by operators: restriction (from a finer to a coarser grid) and prolongation (from a coarser to a finer grid), following a predetermined sequence of meshes. The methods to solve system of equations in a unique mesh are called Singlegrid (SG).

Brandt [14] and Trottenberg et al. [15] investigated several parameters which can be modified in Multigrid method, such as the solver used, the sequence in which each grid is employed defined as Multigrid cycles (V-cycle, W-cycle, F-cycle and others) and the restriction and the prolongation operators. According to the problem's features, the type of information that is transferred among the grids defines Multigrid scheme: the Correction Scheme (CS), in which only the residual is transferred to the coarser grids; or the Full Approximation Scheme (FAS), in which both the residual and the solution are transferred to the coarser grids.

According to Trottenberg et al. [15], studies about Multigrid methods show that the choices of parameters (algebraic or geometric Multigrid, the coarse mesh structure, solver, inner iterations in each mesh, cycles, restriction and prolongation operators, coarsening rate and others) can have a strong influence in the efficiency of the algorithm. There are no general rules in the choice of these parameters, however certain values can be recommended for certain situations. The convergence rate depends on the parameters choices. A simple modification in the algorithm can result in a significant reduction of the CPU time, which justifies the importance of studying the several parameters of Multigrid method.

Meanwhile, the Local Fourier Analysis (LFA) is the main quantitative analysis in order to study the convergence of Multigrid methods and to develop new efficient Multigrid algorithms. This analysis is based on the idea that the error can be expressed as linear combination of the so called Fourier modes. Non-Fourier version can be seen in more details in Karniadakis [16] and Hussaini and Zang [17].

The purpose of this work is to verify the effect of Multigrid method on the CPU time for the resolution of the heat transfer model, based on the Finite Element Method (FEM), in order to simulate the laser surface remelting of the Al–1.5 wt% Fe alloy. To accelerate the convergence of Singlegrid methods, Multigrid method (MG) was employed in order to reduce the CPU time. In this study we analyzed the influence of different geometric Multigrid parameters on the CPU time in the numerical simulation problem. Furthermore, to validate the result of numerical simulation with the experimental result was necessary to perform an analysis of the microstructural characterization of laser-treated layer by the techniques of optical microscopy and SEM.

2 Materials, methods and aspects of the numerical simulation

2.1 Experimental characterization

2.1.1 Preparation of samples

The casting assembly used in solidification experiments consists of water-cooled mold with heat being extracted only from the bottom. It promotes a vertical upward directional solidification and this directional solidification apparatus was used to obtain an Al–1.5 wt% Fe alloy cylindrical casting, with 60 mm diameter and 100 mm length. This alloy was prepared with pure raw materials. Next, 8 mm-wide pieces were cut, polished and sandblasted to reduce their surface reflectance and increase their absorbance for the subsequent laser treatment. The laser surface treatment was performed with a 2 kW Yb-fiber laser (IPG YLR-2000S). The laser beam was focused by a 160 mm lens on the sample surface, while the laser wavelength was $\lambda = 1.06$ μm and the its intensity of the initial moment was $I(0) = 1.81 \times 10^9$ W m^{-2}. The other laser parameters were: a power density of 4.8×10^5 W cm^{-2} with multi-phase distribution of energy with an approximately Gaussian profile, and a scan speed of 40 mm s^{-1}. For this experiment, the sample was positioned 3 mm above the laser focus (out-focusing), using a laser beam diameter of about 600 μm. Experimental works, such as Pariona et al. [1–3] found that the average distance between laser filets was 300 μm and an overlapping of weld filets of about 50 %. This laser treatment without an assisting gas jet was applied to augment the production of metal oxides on the laser-treated surface and to promote the formation of a passive oxide layer in contact with the environment.

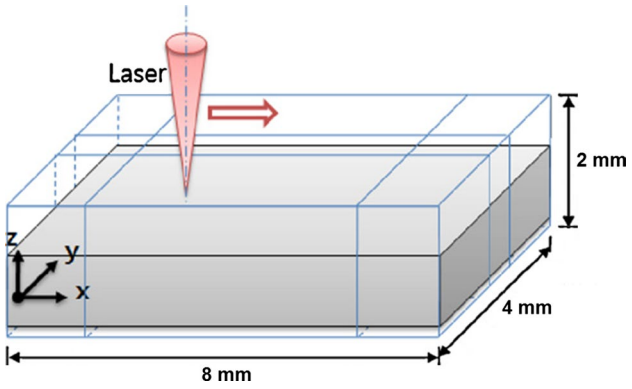

Fig. 1 Schematic view of the laser welding simulation (adapted from Cho et al. [6])

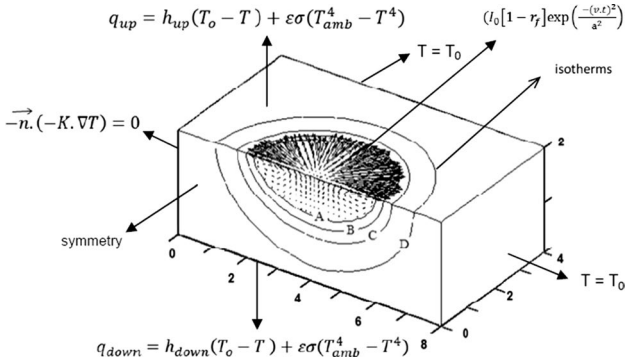

Fig. 2 A 3D computational view of the temperature distribution, including isotherms, for the laser-melted zone, where the initial and boundary conditions are indicated (Adapted from Bag and De [18])

2.1.2 Characterization techniques

For the metallographic characterization (morphological study of the material's structure) of the cross section, small samples were cut and sanded with 600, 800, 1200 grit SiC sand paper, and polished with colloidal silica in a semi-automatic polishing machine (AROTEC Ind. e Com., Brazil). Micrographs were recorded by an optical microscopy (OM, Olympus-BX51) and by a scanning electron microscopy (SEM, Shimadzu SSX-550 microscope).

2.2 Numerical simulation

2.2.1 Numerical simulation by FEM technique

The simulations were carried out with Comsol Multiphysics software, version 4.2, in a microcomputer with Intel™

i7 2.8 GHz processor with 12 GB RAM and Linux operational system. For the simulation procedure a schematic view of the geometry was adopted, as shown in Fig. 1.

The initial and boundary conditions were applied, according to Fig. 2 and the material's thermophysical properties were considered dependent on the temperature and a moving heat source was established in the *x*-axis. The laser parameters used in this work are shown in Table 1.

The thermophysical properties (Thermo-Calc [19], Comsol [20]: density (ρ), thermal conductivity (k) and specific heat (c_p), are shown graphically in Fig. 3. All these properties were determined according to the solidified fraction (Fig. 4a). The enthalpy of this alloy (Fig. 4b) (Thermo-Calc [19]) was necessary to calculate the specific heat. The corresponding heat flux and radiation expressions were applied as boundary conditions as represented in Fig. 2, where: h_{up} is 12.25 W m^{-2} K^{-1}; h_{down} is 6.25 W m^{-2} K^{-1}, these values were used of the literature [21], because, these values were not determined experimentally; ε is the surface emissivity, equals to 0.3; and σ is the Stefan-Boltzmann constant, equals to 5.67×10^{-8} W m^{-2} K^{-4}. The mesh and its respective applied refinement in the sample are displayed in Fig. 5.

2.2.2 *Optimization by Multigrid methods*

For numerical simulation of the laser-treated sample by FEM associated to the Singlegrid method (SG) to solve the systems, which were studied by Hughes [22] and Reddye et al. [23] and a 3D geometric arrangement scheme sample was considered, as presented in Fig. 1. In this work two Singlegrid methods were considered: Multifrontal massively parallel sparse direct solver (Guermouche et al. [24]) and Successive over relaxation (Burden and Faires [25]), which were symbolized by SG-MUMPS and SG-SOR, respectively. These methods were incorporated to improve the numerical simulation of the laser-treatment of Al–1.5 wt% Fe alloy by FEM.

To accelerate the convergence of Singlegrid methods (SG-MUMPS and SG-SOR) Multigrid method (MG) was used. The basic idea is to use a group of meshes of different sizes (different number of elements) alternating the transference of information on each mesh level and the solution of the system of equations in the coarser meshes [11].

Figure 6, illustrates a sequence of meshes that will be used in the coarsening process. In this example, a 33×33 nodes mesh (finest mesh) is considered. The coarsening process was carried out until the 3×3 mesh (coarsest mesh). The amount of employed meshes is called number of levels (L). Figure 6 exemplifies a problem with $L = 5$.

Operators, that transfer information from a fine mesh to the immediately coarser mesh (restriction) and from a coarse mesh to the immediately finer mesh (prolongation), were used. The coarsening ratio (r) is defined as $r = H/h$, where h represent the size of the elements of the fine mesh and H is related to the coarse mesh.

Table 1 Laser parameters used for the mathematical modeling

Welding speed (v)	0.04 m s^{-1}
Real power of laser	600 W
Reflectivity (r_f)	0.63 %
Radius of the Gaussian distribution (a)	3.0×10^{-4} m
Laser peak intensity (I_o)	6.8×10^{9} W m^{-3}
Absorption depth (δ)	Negligible

The systems of equations are solved in each mesh using an iterative method with the purpose of quickly reducing the oscillatory error (smoothing property). Such iterative method is called solver and the number of smoothing steps in a solver (inner iterations), in each level, is symbolized by ν. In this work, when the number of pre-smoothing (smoothing in restriction) and the post-smoothing (smoothing in prolongation) are different, they are called ν_1 and ν_2, respectively.

In Multigrid method several types of cycles (order in which the meshes were used) can be considered. Figure 7 shows some types of cycles, this type of study have been discussed by several authors, such as Trottenberg et al. [15], Ferziger and Peric [26], Reddye and Gartling [23]). Two different types of Multigrid methods can also be defined and they depend on the input data: geometric Multigrid (GMG) and algebraic Multigrid (AMG). In this work, GMG was called as Multigrid method (MG).

3 Results and discussions

3.1 Experimental results

The laser-treated sample micrographs obtained by optical microscopy and scan electron microscopy are shown in Fig. 8. Figure 8a shows by optical microscopy of the surface of the laser-treated sample, where the welding fillets are visible, with an approximated distance of 300 µm between filets. On the surface of the sample are observed different zones, e.g., the weld fillets and the between weld fillets. In the weld fillets zone the morphology is not uniform, where the behavior is more porous than in the between weld fillets zone. In Fig. 8b by optical microscopy is also shown the cross-section of laser processed sample, where in it can be observed the parts of the laser-melt zone and the substrate material, the laser melt zone clearly shows the property of homogenous microstructure, Pariona et al. [1, 2] confirmed this result, which often it presents when the metallic material is laser-treated. A cross-section

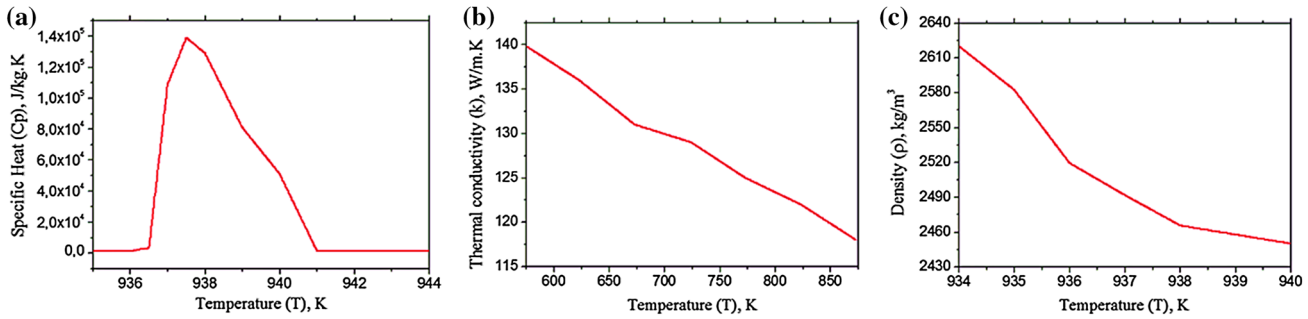

Fig. 3 Thermophysical properties of Al–1.5 wt% Fe alloy: **a** specific heat Cp, **b** thermal conductivity k, and **c** density ρ (Thermo-Calc software [19], Comsol software [21])

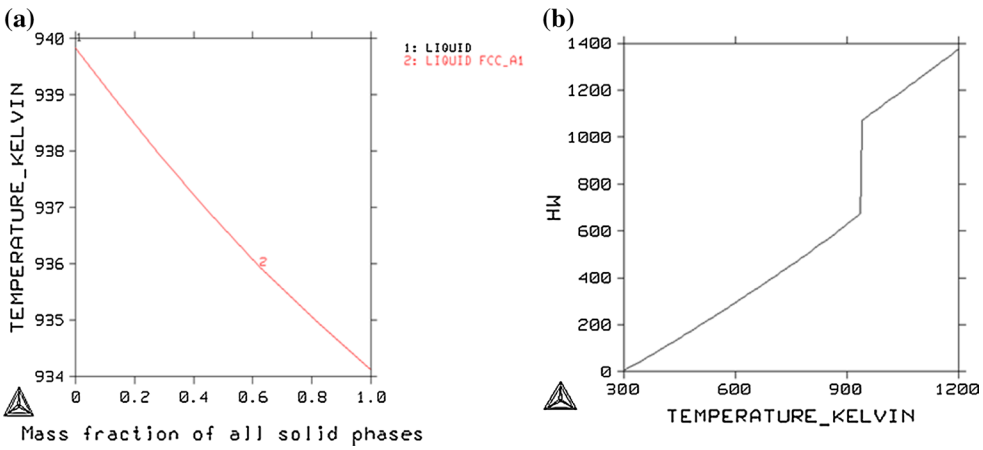

Fig. 4 For the Al–1.5 wt% Fe alloy: **a** solidified fraction and **b** enthalpy (Thermo-Calc software [19])

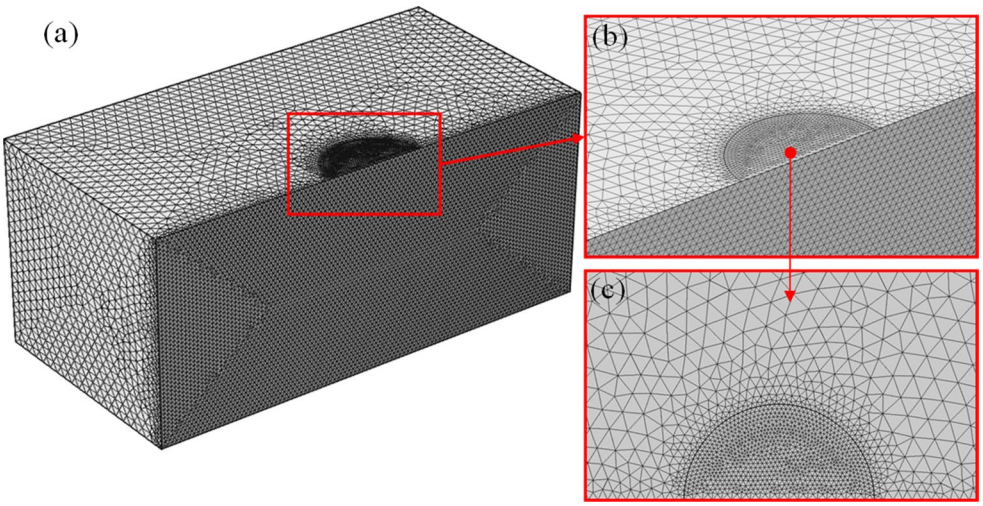

Fig. 5 The mesh and its refinement used in this work: **a** tridimensional view, **b** magnification of details and **c** a top view

image of the laser-treated samples by scan electron microscopy is shown in Fig. 8c, where a homogenous microstructure can be seen more clearly, also in this microstructure are observed the laser melt zone and the substrate material, in the laser-melt zone are observed many nano porosities. In a previous article (Pariona et al. [2]), the characterization of this treated layer was performed and simple metals and metastable intermetallic phases were identified by these authors; the presence of microporosity was also identified, being the largest concentration found on the weld filets. Furthermore, the effect of the laser treatment on the corrosion resistance of LSR-treated and untreated alloy samples

in sulfuric acid (H_2SO_4) 0.1 M at 25 °C was studied by Pariona et al. [2]. For a comparative characterization, the chemically corroded samples were tested using the open circuit potential (OCP), micro and macropolarization techniques. This treatment increased the corrosion resistance 14-fold when compared to the base material of Al–1.5 wt% Fe alloy [2]. The laser treatment on the metal structure produced a chemically and structurally homogenous layer with a fine-grained structure, as can be seen in Fig. 8b, c. These results are coherent with other studies (Pei and Hosson [27], Man et al. [28]) related to investigations of the laser-treated of the Al alloy.

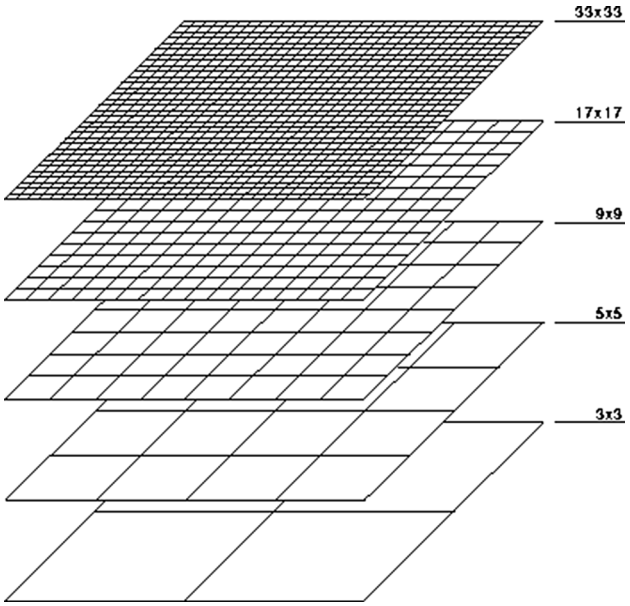

Fig. 6 Process of mesh coarsening and generation

3.2 Numerical results

The FEM simulation was performed based at the conditions of the contour shown in Fig. 2, the mesh was based in Fig. 5 and the thermal physics properties used is shown in Fig. 3, where the laser beam was moved from left to right, at a sweep speed of 40 mm/s. As well, the equation governing the transient heat transfer phenomenon is given by Eq. 1. To display the depth of the laser melted zone (LMZ), the condition of symmetry was applied on the *y* axis.

In Fig. 9a can noted that the isotherms at four different times are not uniformly distributed. In the region located in front of the LMZ, the isotherms are scattered, possibly due to heat energy accumulated through diffusion. On the other hand, in the region situated behind the LMZ presents the lowest scattering of isotherms, this is due to the rapidly cooling which occurs in this region occurs. Yilbas et al. [10] in their research, confirmed that the heat ahead of the LMZ is transferred by conduction, led by a higher thermal gradient. Therefore, the beam is applied on a highly localized area, while the remainder of the material adjacent to the weld fillet is at ambient temperature. Due to this characteristic of the LSR-treated surface, high cooling rates are generated during solidification, which have been studied by Pariona et al. [1] and Su et al. [29]. However in Fig. 9b for the time 0.15 s can be observed with more detail the isotherms, at this figure was highlighted a temperature of 933 K which is near of the eutectic temperature of this system that is 927 K. Therefore for this temperature the liquid phase of Al–Fe turns in $Al_{13}Fe_4$ for cooling in equilibrium.

To optimize the processing time of the simulation was applied Singlegrid method (SG). As a result of this study, Table 2 shows the CPU time (measured in seconds) obtained by the use of SG-MUMPS and SG-SOR methods, for the mesh of Fig. 5. According to the results, it can be verified that SG-SOR is faster than SG-MUMPS. However,

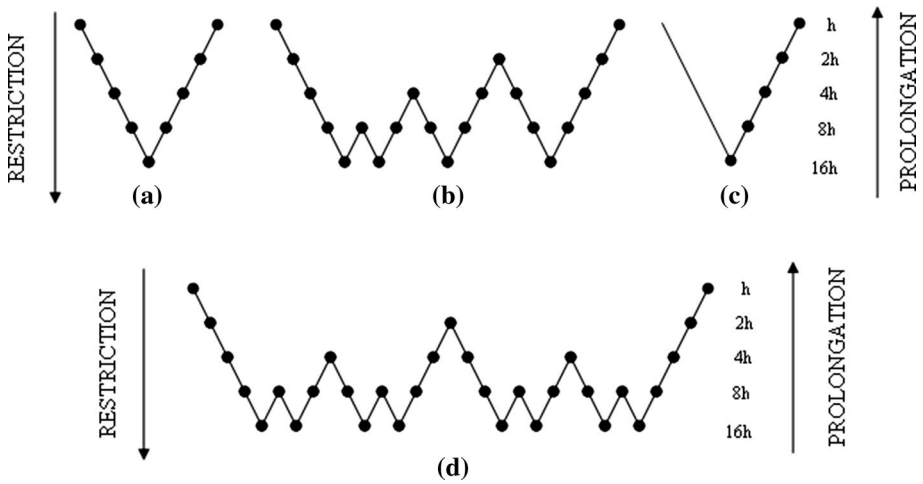

Fig. 7 Diagrams of MG cycles: **a** V-cycle, **b** F-cycle, **c** sawtooth and **d** W-cycle

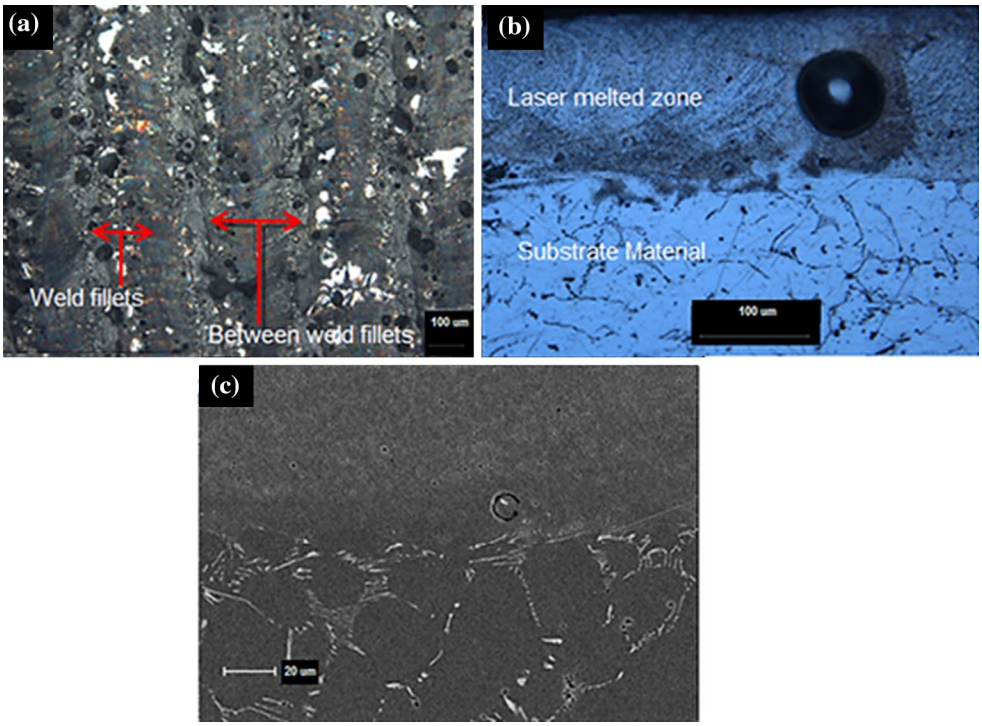

Fig. 8 Microstructural observation in the treated surface and in the cross-section of laser processed sample: **a** optical microscopy of the treated surface, **b** optical microscopy in the cross-section, **c** SEM in the cross-section

the SG-MUMPS is the standard method of Comsol Multiphysics software.

With the purpose of analyze the influence of different geometric Multigrid parameters on the CPU time in the numerical simulation problem; the process of optimization by Multigrid method was applied. Process of optimization is defined here as the minimization process of the CPU time. In this work, CPU time is concerned about the time interval spent for the grids generation (the basis and the auxiliary grids), the appliance of the initial guess, the coefficients evaluation and the solution of the system of linear equations until the achievement of the admitted tolerance.

The employed methodology consists on, for a given the parameter of interest, keeping the other ones with fixed values and, by comparison, choosing the set of parameters is the one that showed the best performance. In this work the simulations with Multigrid method could be split into five categories: type of cycle; number of grids (L); coarsening ratio (r); inner iterations (ν); and solvers. Other methods have been used for comparison, for example: the direct method SG-MUMPS and the iterative method SG-SOR.

As before, like as for the Singlegrid case, the simulations were carried out with Comsol Multiphysics software, however, now with the use of the geometric Multigrid. The standard parameters of geometric Multigrid used were: solver SOR; one inner iteration in the solver ($\nu = 1$); V-cycle Multigrid; and standard mesh coarsening ratio ($r = 2$). Details of parameters of Multigrid method can be found in Trottenberg et al. [15].

For the simulations FEM and triangular grids for mesh were used. For this purpose, four different meshes were considered, with 39,447; 359,719, 987,007 and 2554,531 number of finite element mesh (E). The mesh refinement was focused around the laser source, where the main phenomena of heat affected zone and melting occur.

The most representative results related to the five categories of numerical simulations with Multigrid method are presented below.

3.2.1 Types of cycles

The focus of this subsection is the analysis of the type of cycle which provides the minimum CPU time for a given set of parameters. Some authors like Manzano [30] and Chishlom [31] analyzed the type of cycles in Multigrid method and verified that, in general, a W-cycle gives the best results with respect to CPU time.

In order to reduce the number of numerical simulations, all dependent variables for the CPU time minimization and other standard parameters were fixed. Figure 10 shows the comparison among the V, W and F cycles, because, there is a small improvement of the CPU time on the W-cycle when compared with V and F cycles, consequently this result agrees with the analysis done by the authors Manzano

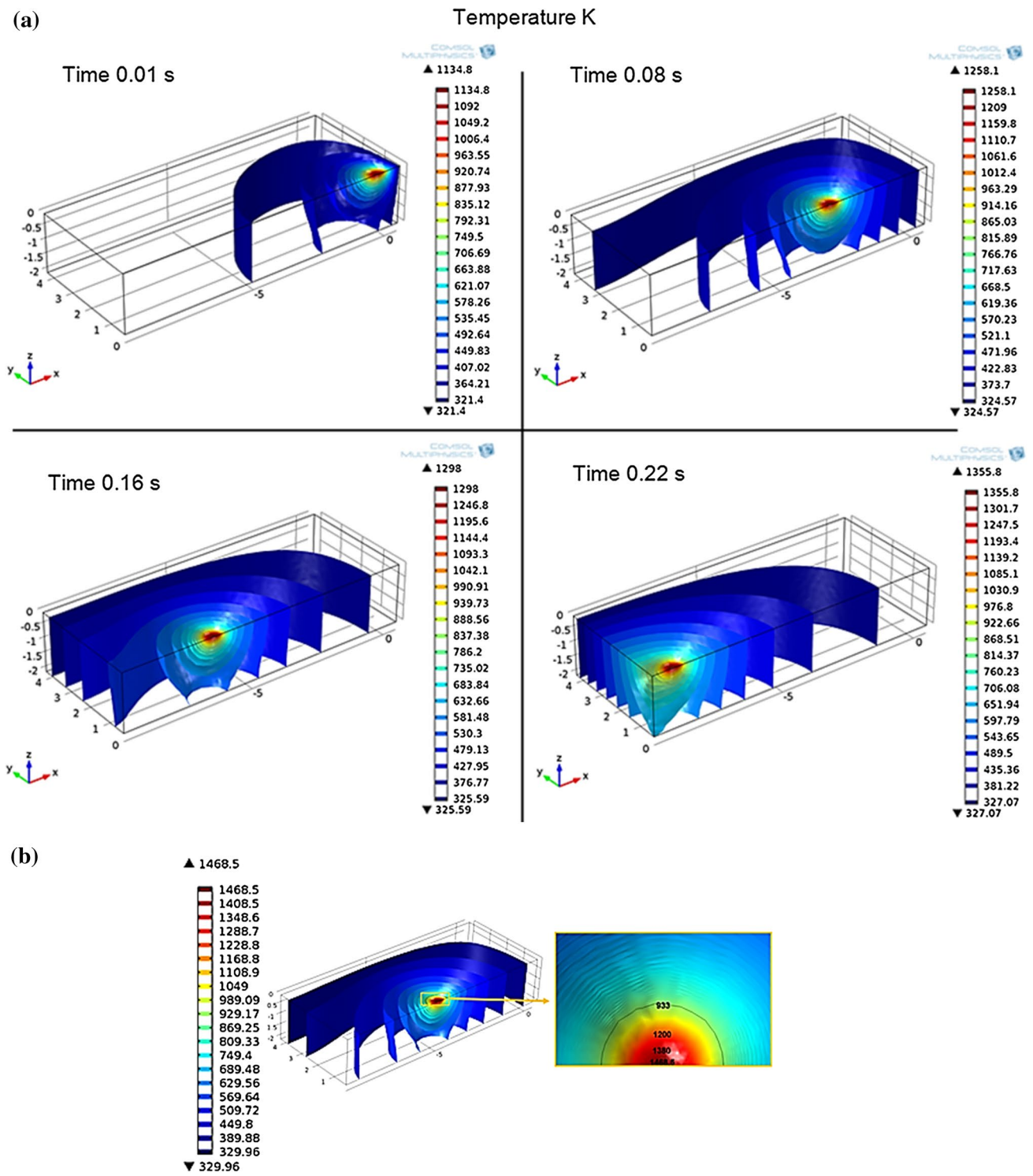

Fig. 9 Numerical simulation during the solidification, showing the pattern of the distribution of the isotherms formed by the LSR treatment: **a** Distribution of the isotherms in mode transient in different instants of time and **b** magnified view of the LMZ for the instant of 0.15 s

[30] and Chishlom [31]. Also on the other hand, the author Chisholm [31] studied the geometric Multigrid for the approximately-Factored implicit Navier–Stokes solver for airfoils and verified that, he has demonstrated in general, a W-cycle gives the fastest results.

Table 2 CPU time for the Singlegrid methods (SG)

Solver	CPU time (s)
SG-MUMPS	7846
SG-SOR	376

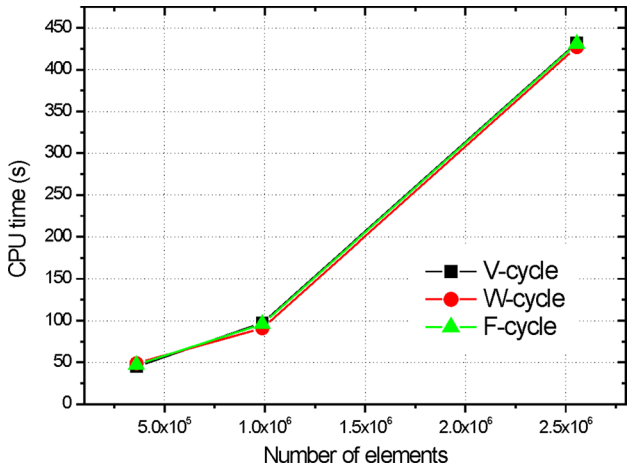

Fig. 10 CPU time versus number of elements

As well, due to the result of Fig. 10 and by studies carried out by the authors that were previously mentioned, the use the W-cycle in this work was adopted.

3.2.2 *Number of levels*

The study of this subsection is the analysis of the number of levels which provides the minimum CPU time for a given set of parameters. Some authors like Suero et al. [32], Oliveira et al. [33], Pinto [34] and Rabi and De Lemos [35] also analyzed the number of levels for problems involving Multigrid method. Figure 11 shows the comparison among the problems with number levels among $L = 1$ (Singlegrid) and $L = 15$. It was verified that, for the data tested, with the increasing of the number of finite element mesh (E), the optimum number of levels is approximated $L = 2$, therefore, the CPU time was less. Note that, in this case, the W-cycle with two levels is reduced to the V-cycle.

3.2.3 *Coarsening ratio*

On the other hand was also investigated the optimum number of coarsening ratio, which provides the minimum CPU time for a given set of components. Pinto [34] also analyzed the coarsening ratio for problems of heat transfer. Figure 12 shows the influence of the coarsening ratio on the CPU time. As the size of the problem increases, it becomes

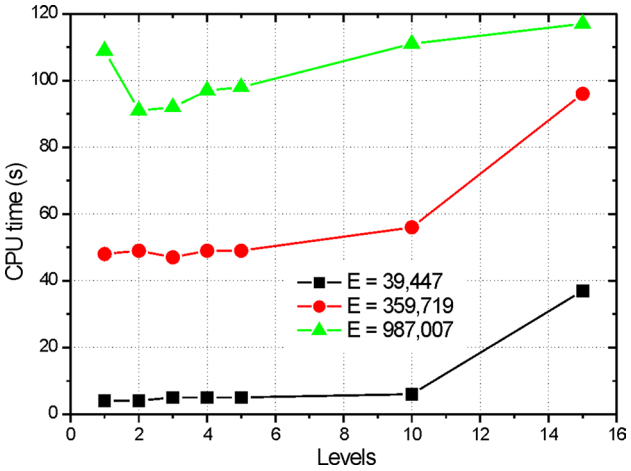

Fig. 11 CPU time versus number of levels

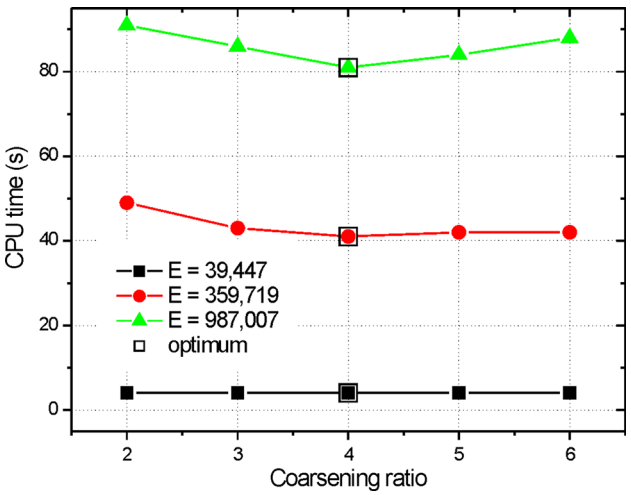

Fig. 12 CPU time versus coarsening ratio

more evident that $r = 4$ is the most efficient coarsening ratio. This result corroborates the Stüben [36] and Moro [37] results.

Stüben [36] developed a study with $r = 2$ and $r = 4$ for unstructured meshes for various two and three-dimensional, linear and nonlinear problems of heat transfer, flow and electromagnetism. In his work, he concluded that $r = 4$ is efficient for anisotropic problems (anisotropy due to the highly stretched meshes). Multigrid method in highly anisotropic meshes was also studied by Oliveira et al. [33]. Moro [37] worked with $r = 2$ and $r = 4$ in structured meshes for a two-dimensional diffusion problem with source term and verified that $r = 4$ was faster than $r = 2$ for the problem under study.

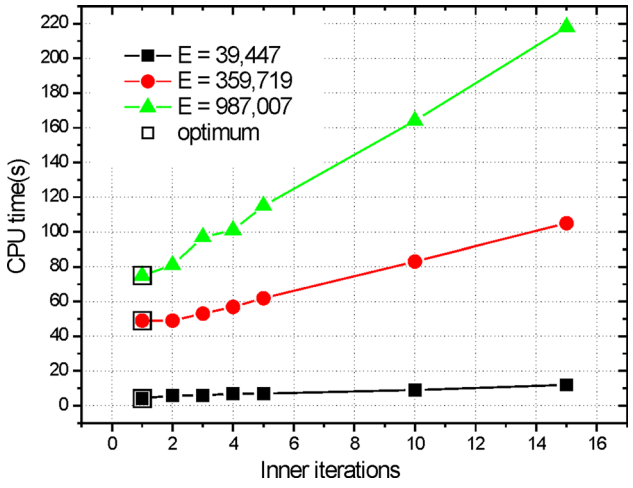

Fig. 13 CPU time versus inner iterations

3.2.4 Inner iterations

In addition, the optimal number of inner iterations (smoothing steps) was studied, which provides the minimum CPU time for a given set of components. Oliveira et al. [33], Gaspar et al. [38] and Rabi and De Lemos [35] also analyzed the optimum number of inner iterations for several problems.

Figure 13 shows the influence of the inner iterations (ν) on the CPU time. It was observed that the minimum CPU time was obtained for $\nu = \nu_1 = \nu_2 = 1$, where ν_1 and ν_2 are the number of pre and post-smoothing, respectively. To study the influence of the size of the linear system of equations, three different values of E (which correspond to three performed discretizations) were used. From this study, it was verified that a small variation in the number of inner iterations increases drastically the CPU time. This result was corroborated by Suero et al. [32] and Gaspar et al. [38]. However, it must be noticed that both groups of authors studied only the Laplace equation. Suero et al. [32] employed the AMG method and Gaspar et al. [38] employed the GMG one.

Another type of tests was also employed, in which the number of inner iterations in the restriction (ν_1) can differ from the number of inner iterations in the prolongation (ν_2). For the tests, ν_1 and ν_2 could vary from 0 to 2. It was observed that the minimum CPU time was obtained with $\nu_1 = 1$ and $\nu_2 = 0$. In literature, this case receives the special name of sawtooth cycle. In this work the sawtooth cycle was applied on the W-cycle.

3.2.5 Comparison between Singlegrid and Multigrid

Hereafter, a comparative study of the performance of the Singlegrid (SG) and Multigrid (MG) methods was performed. The performance of the direct solver MUMPS (SG-MUMPS) and the iterative solvers SOR without Multigrid (SG-SOR), SOR with standard Comsol's Multigrid parameters (SMG-SOR) and SOR with optimizes Multigrid parameters (OMG-SOR) were analyzed. Initially the problem was solved with SG-MUMPS and to compare the methods the speed-up was used.

Table 3 Speed-up (S) of algorithm A in relation to algorithm B

Algorithm A	Algorithm B	S
SG-MUMPS	SG-SOR	20.87
SG-SOR	SMG-SOR	2.46
SG-MUMPS	SMG-SOR	51.28
SMG-SOR	OMG-SOR	2.39
SG-MUMPS	OMG-SOR	122.59

The speed-up of "algorithm A" in relation to "algorithm B" is a measure used to determine the increase of speed obtained during the execution of a program (t_{CPU}) using an algorithm "A" in relation to his execution using an algorithm "B" (Galante [39]). The speed-up is given by the equation:

$$S = \frac{t_{CPU}\ (\text{algorithm A})}{t_{CPU}\ (\text{algorithm B})} \tag{2}$$

Table 3 shows the speed-up for some algorithms. The smallest CPU time was obtained with OMG-SOR. In this study it was verified that OMG-SOR is about 123 times faster than the algorithm SG-MUMPS (standard algorithm of Comsol Multiphysics), which is the used algorithm to simulate the laser surface remelting of the Al–1.5 wt% Fe alloy.

An analysis of relaxations parameters (w) for the solver MG-SOR was also carried out: the relaxation parameter $0 < w < 2$ (under and over relaxation) was tested. In a particular case, when $w = 1$ the SOR method reduces to Gauss–Seidel [25]. According to this analysis, it was verified that the relaxation parameter does not affect significantly the CPU time, therefore the value of $w = 1$ (Gauss–Seidel method) was chosen. Table 4 shows the optimum parameters of Multigrid method obtained in this work.

Through the use of Multigrid method an appreciated reduction in the CPU time was observed. Therefore according to this result was allowed to perform a mesh finer in the geometry in this work, thereby reducing the error tolerance and getting a better precision in the final result.

3.3 An experimental checking

Different analyses of 3D heat transfer by the Finite Element Method (FEM) were conducted in this work, optimized by Multigrid methods. The validation of numerical results was

Table 4 Optimum parameters of Multigrid method

Parameters	Optimum
Type of cycle	W
Number of levels	2
Coarsening ratio	4
Solver	Gauss–Seidel
Inner iteration	$\nu_1 = 1$ and $\nu_2 = 0$

done by the comparison the experimental results of laser-treated sample.

Figure 14 shows the comparison between the experimental result (SEM micrography) and the numerical simulation, where the thermal distributions are indicated by isotherms in the molten pool and as well as in the heat affected zone. The alignment of the figures is different due to the thermal stresses involved in the treated region, in the present study has not considered this phenomenon.

In the micrograph presented in Fig. 14a, a protuberant is observed on the top surface of the laser welding fillet. Bertelli et al. [8] affirmed that this a protuberant was observed when the scanning speed of the laser beam is smaller than 0.03 m s^{-1}. Meanwhile, Teleginski et al. [40] observed that the thermal stress originated from the laser treatment generates strain and deformation on the material surface, due to the sudden heating and melting processes of the laser irradiated region. In this case, only the heat transfer region was considered for the simulations, and therefore Fig. 14b was positioned according to the height of the molten pool. The depth of the molten pool was about 210 μm for 927 Kelvin. According to the Al–Fe phase diagram (Pariona et al. [1]), the eutectic temperature of this system is 927 K, therefore for this temperature the liquid phase of Al–Fe turns in $Al_{13}Fe_4$ for cooling in equilibrium.

4 Conclusions

In the study of the microstructure of the laser-treated sample, on the treated surface were observed different zones of morphologies, for example, on the weld-fillets and between weld-fillets. In the cross-section was observed the cast zone with homogeneous behavior of microstructure and with the presence of many nano porosities. This characteristic of microstructure of the laser-treated sample greatly improves the resistance to corrosion as was shown in the literature.

A transient three dimensional heat transfer problem of the laser remelting process was performed by a numerical simulation with the use of the Finite Element Method (FEM), which allowed the prediction of the temperature distributions in the weld fillet. The CPU time was reduced through the use of Multigrid method (MG) to solve that problem, emphasizing the simulation with the optimum Multigrid (OMG-SOR) is about 122 times faster than the simulation with the MUMPS method (SG-MUMPS). Comparing all numerical studies, the minimum CPU time was obtained with MG and the parameters that have contributed in the optimization, among them were, the number of levels ($L = 2$); the inner iteration in the restriction ($\nu_1 = 1$) and the inner iteration in the prolongation ($\nu_2 = 0$); SOR solver; and the coarsening ratio equals to 4 ($r = 4$).

Multigrid method is a technique very promising of optimization that reduced drastically the CPU time. Because, currently in applied sciences, e.g., in problems of type hybrids within the engineering, when they are simulated which causes long times of CPU. Through the employment of Multigrid technique, the cost of the process of CPU can be very lucrative. For example, in this case applied to laser remelting, a transient problem in 3D with thermophysical property variables was applied Multigrid technique for simulated, since the execution time fall of approximately

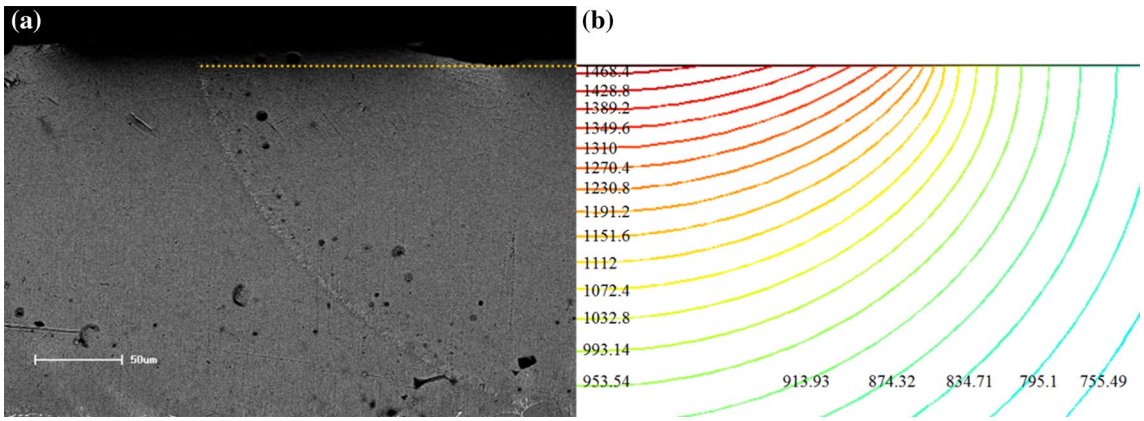

Fig. 14 Comparison between the experimental sample and the numerical simulation, both in the cross section view, where: **a** SEM micrograph and **b** simulation result

6 h to 20 min, which represents the application of this technique very positive. In this study, the experimental result of the microstructural characterization was validated with the result of numerical simulation optimized by the technique of Multigrid method, being that the validation was consistent.

Acknowledgments The authors would like to acknowledge the financial support of the Brazilian research funding agencies: CNPq (Conselho Nacional de Desenvolvimento Científico e Tecnológico, Brazil), FA (Fundação Araucária, Paraná, Brazil) and Dedalo (Development Laboratory of Lasers and Optics Applications) of CTA-IEAv, São José dos Campos, São Paulo, Brazil. The authors would also thank Luciano K. Araki for reviewing the text and for their valuable comments.

References

1. Pariona MM, Teleginski V, Santos K, Machado S, Zara AJ, Zurba NK, Riva R (2012) Yb-fiber laser beam effects on the surface modification of Al–Fe aerospace alloy obtaining weld filet structures, low fine porosity and corrosion resistance. Surf Coat Technol 206:2293–2301. doi:10.1016/j.surfcoat.2011.10.007
2. Pariona MM, Teleginski V, Santos K, Santos ELR, Lima AAOC, Riva R (2012) AFM study of the effects of laser surface remelting on the morphology of Al–Fe aerospace alloys. Mater Charact 74:64–76. doi:10.1016/j.matchar.2012.08.011
3. Pariona MM, Teleginski V, Santos K, Lima AAOC, Zara AJ, Micene KT, Riva R (2013) Influence of laser surface treated on the characterization and corrosion behavior of Al–Fe aerospace alloys. Appl Surf Sci 276:76–85. doi:10.1016/j.apsusc.2013.03.025
4. Miyazaki T, Giedt WH (1982) Heat transfer from an elliptical cylinder moving through an infinite plate applied to electron beam welding. Int J Heat Mass Transf 24:807–814
5. Liu X, Pang M, Zhang ZG, Tan JS, Zhu GX, Wang MD (2012) Numerical simulation of stress field for laser thermal loading on piston. Opt Laser Technol 44:1636–1640. doi:10.1016/j.optlastec.2011.12.045
6. Cho W, Na SJ, Thomy C, Vollertsen F (2012) Numerical simulation of molten pool dynamics in high power disk laser welding. J Mater Process Technol 212:262–275. doi:10.1016/j.jmatprotec.2011.09.011
7. Bessroura ABJ, Masseb J, Bouhafsa M, Barrallier L (2010) Finite element simulation of magnesium alloys laser beam welding. J Mater Process Technol 210:1131–1137. doi:10.1016/j.jmatprotec.2010.02.023
8. Bertelli F, Meza ES, Goulart PR, Cheung N, Riva R, Garcia A (2011) Laser remelting of Al–1.5 wt% Fe alloy surfaces: numerical and experimental analyses. Opt Lasers Eng 49:490–497. doi:10.1016/j.optlaseng.2011.01.007
9. Abderrazak K, Kriaa W, Salem WB, Mhiri H, Lepalec G, Autric M (2009) Numerical and experimental studies of molten pool formation during an interaction of a pulse laser (Nd:YAG) with a magnesium alloy. Opt Laser Technol 41:470–480. doi:10.1016/j.optlastec.2008.07.012
10. Yilbas BS, Arif AFM, Karatas C, Raza K (2009) Laser treatment of aluminum surface: analysis of thermal stress field in the irradiated region. J Mater Process Technol 209:77–88. doi:10.1016/j.jmatprotec.2008.01.047
11. Briggs WL, Henson VE, Mccormick SF (2000) A Multigrid tutorial, 2nd edn. SIAM, Philadelphia
12. Wesseling P (1992) An introduction to Multigrid methods. Wiley, Philadelphia
13. Fedorenko RP (1964) On the speed of convergence of an iteration process. USSR Comput Math Math Phys 4:227–235. doi:10.1016/0041-5553(64)90253-8
14. Brandt A (1977) Multi-level adaptive solutions to boundary-value problems. Math Comput 31:333–390. doi:10.1090/S0025-5718-1977-0431719-X
15. Trottenberg U, Oosterlee CA, Schüller A (2001) Multigrid. Academic Press, St Augustin
16. Karniadakis GE (1990) Spectral element-fourier methods for turbulent flows, computer methods in applied mechanics and engineering. North-Holland 80:367–380
17. Hussaini MY, Zang TA (1987) Spectral methods in fluid dynamics. Ann Rev Fluid Mech 19:339–367
18. Bag S, De A (2010) Computational modelling of conduction mode laser welding process. Laser welding. InTech., Open access. doi:10.5772/256
19. THERMO CALC software (2010) Stockholm, Sweden
20. Users Handbook COMSOL Multiphysics. v. 4.2a (2012)
21. COMSOL Release notes 3.3a (2007) Friction stir welding
22. Hughes TJR (2000) The finite element method—linear static and dynamic finite element analysis. Dover Publications, Mineola
23. Reddye JN, Gartling DK (1994) The finit element method in heat transfer and fluid dynamics. CRC Press, Boca Raton
24. Guermouche A, Yves J, L'Excellent Utard G (2003) Impact of reordering on the memory of a multifrontal solver. Parallel Comput 29:1191–1218. doi:10.1016/S0167-8191(03)00099-1
25. Burden RL, Faires JD (2010) Numerical analysis. Brooks-Cole, 9th edn. Cengage Learning, Australia
26. Ferziger JH, Peric M (2002) Computational methods for fluid dynamics, 3rd edn. Springer, Berlin
27. Pei YY, Hosson JTM (2000) Functionally graded materials produced by laser cladding. Acta Mater 48:2617–2624. doi:10.1002/9781118787694.ch19
28. Man HC, Yang YQ, Lee WB (2004) Laser induced reaction synthesis of TiC + WC reinforced metal matrix composites coatings on Al 6061. Surf Coat Technol 185:74–80. doi:10.1016/j.surfcoat.2003.10.132
29. Su HJ, Zhang J, Ren Q, Deng YF, Liu L, Fu HZ, Soh AK (2013) Laser zone remelting of Al2O3/Er3Al5O12 bulk oxide in situ composite thermal emission ceramics: influence of rapid solidification. Mater Res Bull 48:544–550. doi:10.1016/j.materresbull.2012.11.052
30. Manzano L (1999) Implementation of multigrid for aerodynamic computations on multi-block grids. Dissertation, Department of aerospace science and engineering, University of Toronto
31. Chisholm T (1997) Multigrid acceleration of an approximately-factored algorithm for steady aerodynamic flows. Dissertation, University of Toronto
32. Suero R, Pinto MAV, Marchi CH, Araki LK, Alves AC (2012) Analysis of algebraic Multigrid parameters for two-dimensional steady-state heat diffusion equations. Appl Math Model 36:2996–3006. doi:10.1016/j.apm.2011.09.088
33. Oliveira F, Pinto MAV, Marchi CH, Araki LK (2012) Optimized partial semicoarsening Multigrid algorithm for heat diffusion problems and anisotropic grids. Appl Math Model 36:4665–4676. doi:10.1016/j.apm.2011.11.084
34. Pinto MAV (2006) Multigrid method behavior problems in heat transfer. PhD Thesis, UFPR, Curitiba, PR-Brazil
35. Rabi JA, De Lemos MJS (1998) The Effects of Peclet number and cycling strategy on Multigrid numerical solutions of convective-advective problems. In: 7th, AIAAIASME international thermics and HT conference, Paper AIAA-98-2584, Albuquerque, New Mexico, USA

36. Stüben K (1999) Algebraic Multigrid (AMG): an introduction with applications. In: GMD-report 70
37. Moro Filho RC (2004) Technical application of multigrid in computational heat transfer, XXV Iberian Latin_American congress on computational methods in engineering
38. Gaspar FJ, Gracia JL, Lisbona FJ, Rodrigo C (2009) On geometric Multigrid methods for triangular grids using three-coarsening strategy. Appl Numer Math 59:1693–1708. doi:10.1016/j.apnum.2009.01.003
39. Galante G (2006) Parallel Multigrid methods on structured meshes non-simulation applied problems of computational fluid dynamics na heat transfer. Dissertation UFRGS, Porto Alegre, RS, Brazil
40. Teleginski V, Riva R, Pariona MM (2012) Avaliação do estresse térmico no tratamento de refusão superficial a laser da liga Al–1.5% Fe através da técnica dos elementos finitos. In: 67º Congresso ABM, 2012, Rio de Janeiro. Anais do 67º Congresso Anual da ABM 3518–3527